

## Nonconservation of the Valley Density and Its Implications for the Observation of the Valley Hall Effect

Alexander Kazantsev<sup>1,\*</sup>, Amelia Mills,<sup>1</sup> Eoin O'Neill<sup>1</sup>, Hao Sun,<sup>2</sup> Giovanni Vignale,<sup>2</sup> and Alessandro Principi<sup>1,†</sup>

<sup>1</sup>*Department of Physics and Astronomy, University of Manchester, Manchester M13 9PL, United Kingdom*

<sup>2</sup>*The Institute for Functional Intelligent Materials (I-FIM), National University of Singapore,  
4 Science Drive 2, Singapore 117544, Singapore*



(Received 15 December 2022; revised 10 October 2023; accepted 26 January 2024; published 4 March 2024)

We show that the conservation of the valley density in multivalley insulators is broken in an unexpected way by the electric field that drives the valley Hall effect. This implies that time-reversal-invariant fully gapped insulators, in which no bulk or edge state crosses the Fermi level, can support a valley Hall current in the bulk and yet show no valley density accumulation at the edges. Thus, the valley Hall effect cannot be observed in such systems. If the system is not fully gapped then valley density accumulation at the edges is possible. The accumulation has no contribution from undergap states and can be expressed as a Fermi surface average, for which we derive an explicit formula. We demonstrate the theory by calculating the valley density accumulations in an archetypical valley-Hall insulator: a gapped graphene nanoribbon. Surprisingly, we discover that a net valley density polarization is dynamically generated for certain edge terminations.

DOI: [10.1103/PhysRevLett.132.106301](https://doi.org/10.1103/PhysRevLett.132.106301)

*Introduction.*—The valley Hall effect (VHE) in non-topological systems has recently stirred considerable controversy [1–9]. When the band structure features two valleys with a nonvanishing Berry curvature, electrons skew in the direction orthogonal to the applied electric field, even without a magnetic field. However, since the system is not topological, electrons from the two valleys skew in opposite directions giving rise to a zero (charge) Hall current but a finite *valley* Hall current  $\mathbf{j}_v(\mathbf{r}, t)$ . This is defined as the difference between charge currents of electrons originating in opposite valleys. When this current hits the edge of the system, a valley density  $n_v(\mathbf{r}, t)$  (or, more physically, orbital magnetization [10]), is expected to accumulate at its boundaries. This assumes that the valley density obeys a standard continuity equation [5,6]. This seems a reasonable assumption: the two valleys are well separated in momentum space, up to the point that they could ideally be taken as completely disconnected.

Some authors [1,6] went further and claimed that even a fully gapped nontopological insulator such as graphene aligned with hexagonal boron nitride (hBN) [3,4] can exhibit nonlocal charge transport mediated by transverse bulk undergap valley currents. The authors of Ref. [6] argued that, at finite temperature, the valley-density

accumulation could drive a “squeezed edge current” (parallel to the edges) in apparent agreement with experiment [2]. However, other authors [7–9] found from microscopic calculations no valley density accumulation or edge current in the simple graphene/hBN model. In the case of a *fully gapped insulator*, in which no bulk or edge state crosses the Fermi level, this leaves us with the following puzzle: on one hand, the electric field drives a finite dissipationless valley Hall current in the bulk; on the other hand, time reversal symmetry implies that a valley density accumulation—a time-reversal-odd quantity—cannot appear in response to an electric field, unless there is dissipation, which is impossible with no states at the Fermi level. So where did the valley current go?

In this Letter we solve the puzzle by observing that valley density does not satisfy a conventional continuity equation when an electric field is present. The reason is that the electric field breaks the conservation of crystal momentum and therefore of valley number, which depends explicitly on it. As a result, the bulk valley current is internally short-circuited as electrons flow from one valley to the other (and thus switch the sign of the Berry curvature) under the action of the very same electric field that drives the valley Hall current in the first instance. This process is schematically shown in Fig. 1.

Our results imply that in a (i) time-reversal invariant (ii) fully gapped insulator, as defined above, the undergap valley current cannot produce a valley density accumulation at the edge. This holds irrespective of the presence or absence of spin-orbit coupling as long as the two conditions above are met and applies equally well to systems based on

Published by the American Physical Society under the terms of the [Creative Commons Attribution 4.0 International license](https://creativecommons.org/licenses/by/4.0/). Further distribution of this work must maintain attribution to the author(s) and the published article's title, journal citation, and DOI.

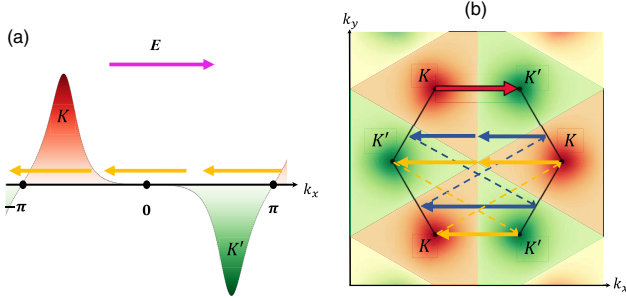


FIG. 1. Panel (a): The cyclic flow of electrons (yellow arrows) in the one-dimensional Brillouin zone of a ribbon subject to electric field  $E$  (pink arrow). The valley charge changes sign whenever the electron crosses the boundaries between the red and green regions ( $k_x = 0, \pm\pi$ ). Each electron performs half the cycle as a “left-valley electron” and half as a “right-valley electron.” Also shown are the Berry curvature hot spots with a positive (negative) value near  $K$  ( $K'$ ). Because of opposite Berry curvatures in the two valleys, the result is a steady valley Hall current. However, in a fully gapped insulator, at the end of the cycle each electron returns to its initial state, thus no valley redistribution occurs. Panel (b): Two examples (blue and yellow arrows) of a similar flow in the two-dimensional Brillouin zone of the infinite system.

graphene or transition metal dichalcogenides. This makes observing the VHE impossible in such systems unless, e.g., the valley degeneracy is lifted [11–13] or carriers are selectively injected into a single valley [14]. In these cases, an electric (not valley) charge density is detected due to a nonzero net anomalous Hall effect. This is distinct from the VHE that was originally discussed in Refs. [1–3] and for which the controversy exists. Our result also implies that the nonlocal transport detected in Refs. [1,15–18] must have been caused by partially occupied bulk or edge bands.

In metallic systems, which support a Fermi surface, our predictions are quite different from those of the conventional theory which assumes valley number conservation. In particular, in our theory the accumulation depends on the form of the electronic wave functions near the edge. The length over which it occurs is not related to the carrier diffusion length as in, e.g., Ref. [5], but reflects the much shorter localization length of edge states, as observed in some experiments [19], or the Fermi wavelength of bulk states. Perhaps the most important result of this study is that valley density of equal sign can be generated on both edges simultaneously [20].

*Summary of main ideas.*—We consider a generic system in the shape of a strip of finite width that is indefinitely extended along the  $x$  axis. As we show below, the continuity equation satisfied by the valley density is

$$\partial_t n_v(y, t) + \partial_y J_v^y(y, t) = -e^2 E(t) \sum_k S(k) \partial_k f_k(y), \quad (1)$$

where the electric field is in the  $x$  direction, which is parallel to the edge, and the valley current is in the  $y$

direction, perpendicular to the edge. Edges are chosen to be parallel to one of the vectors connecting the two valleys in the Brillouin zone of the infinite system. One such vector (one of six) is shown in Fig. 1(b) with a red arrow. We call  $k_x$  its direction in momentum space and  $x$  in real space. In a strip,  $k_x$  remains a good quantum number and serves as Bloch momentum in the one-dimensional Brillouin zone. For brevity, in what follows we will drop subscript “ $x$ ” on  $k_x$ . The electronic states (in the absence of the electric field) have the form  $\psi_{k,n}(x, y) = e^{ikx} u_{k,n}(x, y) / \sqrt{2\pi}$ , where  $n$  is the band index. The sum over  $k$  in Eq. (1) stands for  $\int dk / (2\pi)$ . The mixed electronic distribution  $f_k(y) = a^{-1} \int_0^a dx \sum_n f_{k,n} |u_{k,n}(x, y)|^2$  is defined in terms of the electronic wave functions and the occupations of the corresponding states  $f_{k,n}$ , with the integral taken over one period  $a$  in the  $x$  direction.  $S(k)$  is a “valley charge” function (odd under time reversal), which is a smooth periodic function of  $k$  in the Brillouin zone. It assigns number  $+1$  to states around one valley and  $-1$  to states around the other valley. The valley density operator is  $\hat{n}_v(\mathbf{r}) \equiv -(e/2) \sum_j \{S(\hat{k}_j), \delta(\mathbf{r} - \hat{\mathbf{r}}_j)\}$ , where  $\hat{\mathbf{r}}_j$  and  $\hat{k}_j$  are the position and Bloch momentum operator (along the edge) of the  $j$ th electron, respectively, and  $\{\hat{A}, \hat{B}\} \equiv (\hat{A}\hat{B} + \hat{B}\hat{A})$ . The valley current density is  $\hat{\mathbf{j}}_v(\mathbf{r}) \equiv -(e/4) \sum_j \{S(\hat{k}_j), \{\hat{\mathbf{v}}_j, \delta(\mathbf{r} - \hat{\mathbf{r}}_j)\}\}$ , where  $\hat{\mathbf{v}}_j$  is the velocity operator. Since  $\hat{k}$  is conserved,  $\hat{n}_v$  and  $\hat{\mathbf{j}}_v(\mathbf{r})$  obey a conventional continuity equation in the absence of the electric field.

As shown below, in a fully gapped time-reversal invariant insulator, in which no edge or bulk state crosses the Fermi level, and at zero temperature, the right-hand side of Eq. (1) completely cancels the contribution due to the current on the left-hand side. Thus, the valley density accumulation vanishes, even though there is a finite valley current in the bulk. In all other cases the cancellation is not exact. The correct equation for the density accumulation rate in the absence of relaxation processes is then  $\partial_t n_v(y, t) = -Q_s(y)$ , where the source term

$$Q_s(y) = \frac{e^2 E}{a} \int_0^a dx \sum_{k,n} (\partial_k f_{k,n}) S(k) |u_{k,n}(x, y)|^2, \quad (2)$$

is a Fermi surface property. Note that  $Q_s(y)$  cannot be written, in general, as the divergence of a current. In fact, this is only possible if its integral across the strip vanishes, which implies that density accumulates at one edge and depletes at the other [21]. However, if the width of the strip is macroscopically large, the source term is localized on the edges. One can then define the “effective current”  $I_s$ , obtained by integrating Eq. (2) across a given edge, that feeds the valley number accumulation thereat. It can be split as  $I_s = I_s^e + I_s^b$ , where  $I_s^e = e^2 E \sum_{k,e} (\partial_k f_{k,e}) S(k)$  is the contribution of the edge states. Here, the sum over  $e$  is that

over the edge states. The contribution of the bulk states,  $I_s^b$ , can be obtained in terms of the probability amplitude for the propagating Bloch waves to scatter off the edge [see Eq. (6) below]. Once  $I_s$  is known, the valley number accumulation can be estimated as  $I_s \tau_{lr}$ , where  $\tau_{lr}$  is the intra- or intervalley momentum relaxation time for the bulk or edge states' contribution, respectively.

*Anomalous continuity equation.*—We consider a 2D crystal periodic in the  $x$  direction with period  $a = 1$  and with the edges positioned at  $y = 0$  and  $y = -W$ . A uniform electric field of magnitude  $E$  oscillating at frequency  $\omega$  is applied along the  $x$  direction. For conciseness, hereafter we set  $\hbar = 1$ . Thus the conductance quantum  $e^2/h$  equals  $e^2/(2\pi)$ , where  $e$  is the electron charge. From the Kubo formula [23,24], the  $y$  component of the valley current (averaged over  $x$ ) is [25]

$$j_v^y(y, \omega) = iEe^2 \sum_{k,n,n'} \int_0^y dy' (\varepsilon_{k,n} - \varepsilon_{k,n'}) \times S(k) \mathcal{L}_{k,nn'}(\omega) \mathcal{W}_{k,nn'}(y') \mathcal{A}_{k,n'n}, \quad (3)$$

and the valley density (also averaged over  $x$ )

$$n_v(y, \omega) = -\frac{iEe^2}{\omega + i0} \sum_{k,n} (\partial_k f_{k,n}) S(k) \mathcal{W}_{k,nn}(y) - Ee^2 \sum_{k,n,n'} S(k) \mathcal{L}_{k,nn'}(\omega) \mathcal{W}_{k,nn'}(y) \mathcal{A}_{k,n'n}, \quad (4)$$

where  $\mathcal{L}_{k,nn'}(\omega) \equiv (f_{k,n} - f_{k,n'})/(\omega + \varepsilon_{k,n} - \varepsilon_{k,n'} + i0)$  is the usual Lindhard factor [24],  $\mathcal{W}_{k,nn'}(y) \equiv \int_0^1 dx u_{k,n}^\dagger(x, y) u_{k,n'}(x, y)$ , and  $\mathcal{A}_{k,n'n} = \int_0^1 dx \int_{-W}^0 dy \times u_{k,n'}^\dagger(x, y) i\partial_k u_{k,n}(x, y)$  is the Berry connection. The Fourier transform of Eq. (1) follows directly [25] from Eqs. (3) and (4):

$$-i\omega n_v(y, \omega) + \partial_y j_v^y(y, \omega) = -e^2 E \sum_k S(k) \partial_k f_k(y). \quad (5)$$

*The vanishing of valley density accumulation.*—Let us first assume that the system is a time-reversal invariant fully gapped insulator, such that no bulk or edge state crosses the Fermi level. The first term on the right-hand side of Eq. (4) vanishes because  $\partial_k f_{k,n} = 0$ , since no band crosses the Fermi level. Because of time-reversal symmetry, the second line on the right-hand side of Eq. (4) is proportional to  $\omega$  [25], so the valley density accumulation vanishes for a static electric field. This result implies that  $\partial_y j_v^y(y)$  can be different from zero—as it must necessarily be, since the valley Hall current is finite in the bulk but vanishes at the edges—yet this finite divergence does not cause any density change at the edge or anywhere else. The resolution of this paradox is provided by the anomalous term on the right-hand side of Eq. (1) which exactly matches the

divergence term on the left-hand side when the system is fully gapped.

*The source of valley density.*—Let us now consider the case in which the system is not fully gapped and some states cross the Fermi level. Then the cancellation between the anomalous term and divergence of the current is not perfect. Indeed, the first term on the right-hand side of Eq. (4) causes the density to grow at a constant rate, leading to a breakdown of linear response theory unless a limiting momentum relaxation mechanism is taken into account. The Fermi surface term, obtained by multiplying Eq. (4) by  $-i\omega$  and taking the  $\omega \rightarrow 0$  limit, is the “source term”  $Q_s(y)$  in Eq. (2). It receives contributions from both bulk and edge states, both decaying away from the edge, the latter exponentially and the former oscillating at half the Fermi wavelength. As discussed above, the integral of  $Q_s(y)$  over  $y$  across a single edge can be interpreted as an effective current  $I_s$  that feeds the density accumulation thereat. The contribution of bulk states to  $I_s$  is (at  $y = 0$ )

$$I_s^b = -2e^2 E \sum_{\lambda, k, p > 0} \partial_k f_{k,p}^\lambda \mathfrak{Im} \left[ \frac{[v_{k,p}^\lambda]^\dagger v_{k,-p}^\lambda R_\lambda(k, p)}{p + i0} \right], \quad (6)$$

where momentum integration is restricted to the valley with valley number  $+1$ ,  $p$  is momentum in the  $y$  direction measured from the valley bottom,  $v_{k,p}^\lambda$  are envelope amplitudes of propagating stationary states, labeled by index  $\lambda$ ,  $R_\lambda(k, p)$  is the reflection probability amplitude ( $|R_\lambda(k, p)| = 1$ ) (see [25] for details).

*Example: “gapped graphene.”*—To illustrate the general theory developed above, we calculate the valley Hall current and valley density accumulation rate for a nanoribbon of “gapped graphene”—a model system that captures some aspects of monolayer graphene on a gap-inducing hBN substrate. For the nanoribbon we consider two terminations: (a) zigzag boundaries on both edges [Fig. 2(a)] and (b) a zigzag and a bearded edge [Fig. 2(c)]. Each unit cell, labeled by an integer  $l$ , contains  $N$  horizontal rows, each labeled by an integer  $m$ . Each row contains two atoms of sublattices  $A$  and  $B$  as shown in Fig. 2(a), except the edge rows, where one atom may be missing as shown in Fig. 2(c). The two sublattices,  $A$  and  $B$ , have different on-site potentials  $\pm\Delta$ . Electrons are assumed to hop only between nearest neighbors. We neglect spin-orbit interaction and therefore consider spinless electrons. The  $y$  coordinate will take integer values to indicate the row and half-integer values to mark the position halfway between the rows.

The band structures for the two terminations, shown in Figs. 2(b) and 2(d), respectively, feature two bulk bands separated by a gap equal to  $2|\Delta|$  with minima at  $k = \pm 2\pi/3$ . These points define the two valleys in the one-dimensional Brillouin zone. The blue lines show bands of edge states.

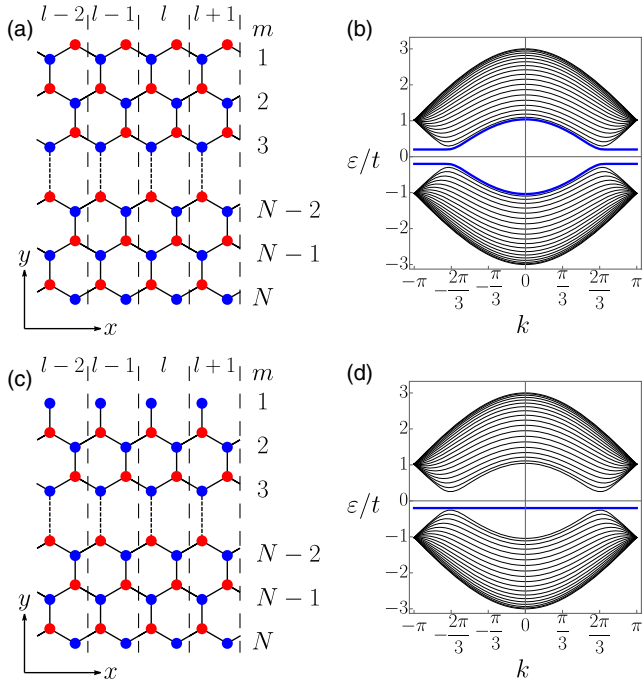


FIG. 2. Panel (a) and (c): Gapped graphene nanoribbon with two zigzag edges and a zigzag and a bearded edge (at the top), respectively. Red (blue) discs signify atoms of the A (B) sublattice. Panel (b) and (d): Band structures of nanoribbons of panels (a) and (c), respectively, for  $N = 20$  and  $\Delta = 0.2t$ .

Our main results are presented in Fig. 3. For a Fermi energy in the gap ( $\epsilon_F = 0$ ) and at zero temperature, we find that  $n_v(m, 0) = 0$  for either termination, consistent with the absence of states at the Fermi level. At the same time  $j_v^y(m + 1/2, 0) = -Ee^2 \cdot \text{sign}(\Delta)/(2\pi) + O(\Delta/t)$  for  $1 \leq m \leq N - 1$  as shown in panels (a) and (b), blue line: this is the undergap current associated with the nearly-quantized Hall conductance (the actual value  $-0.9$  deviates from the ideal quantized value  $-1$  due to the finite bandwidth of the model) [25].

When the system is doped, the current distributions differ dramatically for the two terminations, as shown by the red lines in Figs. 3(a) and 3(b). In the case of the double zigzag termination the current shows a linear variation across the ribbon [red line in (a)], changing sign about the center of the ribbon. This is contrary to our intuition, which would suggest an approximately constant current in the bulk. Of greater physical interest, however, is the valley density accumulation rate shown in Fig. 3(c). There is a significant cancellation between  $-\partial_y j_v^y$  (green line) and the nonconservation term (black line) at the edges. Their sum results in a density accumulation rate displaying oscillations (red dots) on the scale of half the Fermi wavelength and two spikes of equal signs at the edges. The fact that the accumulation rate does not integrate to zero is the result of the anomaly on the right-hand side of Eq. (1): valley number is pumped from one valley into the other via a

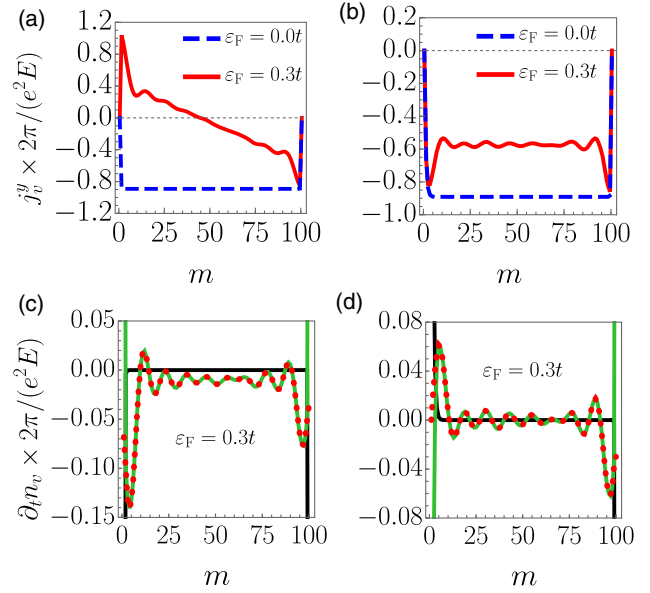


FIG. 3. Panel (a): Gapped graphene nanoribbon with zigzag edges: the blue dashed (red solid) line shows the valley Hall current as a function of position at Fermi energy  $\epsilon_F = 0$  ( $\epsilon_F = 0.3t$ ). Panel (b): Same as in (a) for a nanoribbon with one zigzag and one bearded edge. Panel (c): Contribution to the valley density accumulation rate from the valley Hall current (green), from the nonconservation term (black), and their sum, i.e., the total accumulation rate (red dotted), in the nanoribbon with zigzag edges. Panel (d): Same as in (c) for the nanoribbon with one zigzag and one bearded edge. In all plots  $N = 100$ ,  $\Delta = 0.1t$ . In plots (c) and (d)  $\epsilon_F = 0.3t$ .

partially filled band of edge states connecting the two [upper blue line in Fig. 2(b)]. This opens an intriguing possibility of generating a net valley density polarization by purely electrical means, as opposed to the standard optical methods. Note, however, that the form of valley density accumulation rate cannot be predicted from the valley Hall current alone and depends on the boundary conditions. Because valley number and orbital magnetic moment are closely related [10], the same effect should emerge for orbital magnetization, as was indeed found in Ref. [28].

The zigzag + bearded termination presents us with a more familiar scenario. Figure 3(b) shows that the valley Hall current is approximately constant [ $-0.55$  in units of  $e^2 E/(2\pi)$  at  $\epsilon_F = 0.3t$ ] in the bulk. At the same time the valley density accumulation rate [panel (d)] has spikes of opposite signs on the two edges (red dots). In this case, valley density is transported from one edge to the other. The reason for the overall valley number conservation is, in contrast to the previous example, absence of partially filled bands connecting the two valleys.

*Conclusion.*—The modified continuity equation (1) allows us to explain how a nonvanishing undergap valley current can coexist with a vanishing valley density accumulation in a fully gapped nontopological time-reversal-invariant system with perfectly degenerate valleys. Any

valley density accumulation requires the existence of states at the Fermi level and furthermore it is a dissipative process that requires a scattering mechanism to reach a steady state. We have provided closed expressions for calculating valley density accumulation rates on the edges of a two-dimensional material and we have applied them to the gapped graphene model: these formulas show that the connection between bulk currents and measurable edge accumulations is much more complex than previously suspected. This, in particular, leads us to surmise that any physical system in which evidence of the VHE has been found either by Kerr rotation microscopy [29] or by nonlocal resistance measurements [1,15–18] cannot be a true insulator but must have partially populated bulk or edge states.

A. P. acknowledges support from the European Commission under the EU Horizon 2020 MSCA-RISE-2019 programme (project 873028 HYDROTRONICS). A. P. and A. K. acknowledge support from the Leverhulme Trust under the Grant No. RPG-2019-363. H. S. and G. V. were supported by the Ministry of Education, Singapore, under its Research Centre of Excellence award to the Institute for Functional Intelligent Materials (I-FIM, Project No. EDUNC-33-18-279-V12).

\*alexander.kazantsev@manchester.ac.uk

†alessandro.principi@manchester.ac.uk

- [1] R. V. Gorbachev, J. C. W. Song, G. L. Yu, A. V. Kretinin, F. Withers, Y. Cao, A. Mishchenko, I. V. Grigorieva, K. S. Novoselov, L. S. Levitov, and A. K. Geim, *Science* **346**, 448 (2014).
- [2] M. J. Zhu, A. V. Kretinin, M. D. Thompson, D. A. Bandurin, S. Hu, G. L. Yu, J. Birkbeck, A. Mishchenko, I. J. Vera-Marun, K. Watanabe, T. Taniguchi, M. Polini, J. R. Prance, K. S. Novoselov, A. K. Geim, and M. Ben Shalom, *Nat. Commun.* **8**, 14552 (2017).
- [3] Y. D. Lensky, J. C. W. Song, P. Samutpraphoot, and L. S. Levitov, *Phys. Rev. Lett.* **114**, 256601 (2015).
- [4] D. Xiao, W. Yao, and Q. Niu, *Phys. Rev. Lett.* **99**, 236809 (2007).
- [5] M. Beconcini, F. Taddei, and M. Polini, *Phys. Rev. B* **94**, 121408(R) (2016).
- [6] J. C. W. Song and G. Vignale, *Phys. Rev. B* **99**, 235405 (2019).
- [7] J. M. Marmolejo-Tejada, J. H. García, M. D. Petrović, P.-H. Chang, X.-L. Sheng, A. Cresti, P. Plecháč, S. Roche, and B. K. Nikolić, *J. Phys.* **1**, 015006 (2018).
- [8] S. Roche, S. R. Power, B. K. Nikolić, J. H. García, and A.-P. Jauho, *J. Phys.* **5**, 021001 (2022).
- [9] T. Aktor, J. H. Garcia, S. Roche, A.-P. Jauho, and S. R. Power, *Phys. Rev. B* **103**, 115406 (2021).
- [10] S. Bhowal and G. Vignale, *Phys. Rev. B* **103**, 195309 (2021).
- [11] W. Du, R. Peng, Z. He, Y. Dai, B. Huang, and Y. Ma, *npj 2D Mater. Appl.* **6**, 11 (2022).
- [12] X. Ma, X. Shao, Y. Fan, J. Liu, X. Feng, L. Sun, and M. Zhao, *J. Mater. Chem. C* **8**, 14895 (2020).
- [13] B. Zhou, Z. Li, J. Wang, X. Niu, and C. Luan, *Nanoscale* **11**, 13567 (2019).
- [14] K. F. Mak, K. L. McGill, J. Park, and P. L. McEuen, *Science* **344**, 1489 (2014).
- [15] M. Sui, G. Chen, L. Ma, W.-Y. Shan, D. Tian, K. Watanabe, T. Taniguchi, X. Jin, W. Yao, D. Xiao, and Y. Zhang, *Nat. Phys.* **11**, 1027 (2015).
- [16] K. Endo, K. Komatsu, T. Iwasaki, E. Watanabe, D. Tsuya, K. Watanabe, T. Taniguchi, Y. Noguchi, Y. Wakayama, Y. Morita, and S. Moriyama, *Appl. Phys. Lett.* **114**, 243105 (2019).
- [17] Y. Shimazaki, M. Yamamoto, I. V. Borzenets, K. Watanabe, T. Taniguchi, and S. Tarucha, *Nat. Phys.* **11**, 1032 (2015).
- [18] E. Arrighi, V. H. Nguyen, M. D. Luca, G. Maffione, Y. Hong, L. Farrar, K. Watanabe, T. Taniguchi, D. Maily, J. C. Charlier, and R. Ribeiro-Palau, *Nat. Commun.* **14**, 8178 (2023).
- [19] I. Lyalin, S. Alikhah, M. Berritta, P. M. Oppeneer, and R. K. Kawakami, *Phys. Rev. Lett.* **131**, 156702 (2023).
- [20] Since valley number is closely related to orbital magnetic moment [10] we expect similar results for orbital magnetization.
- [21] A similar situation was discussed in Ref. [22] for the spin current, with the difference that there the nonconservation of spin density was caused by an intrinsic spin-orbit torque, while here it is caused by the very same electric field that drives the valley Hall effect.
- [22] J. Shi, P. Zhang, D. Xiao, and Q. Niu, *Phys. Rev. Lett.* **96**, 076604 (2006).
- [23] R. Kubo, *J. Phys. Soc. Jpn.* **12**, 570 (1957).
- [24] G. Giuliani and G. Vignale, *Quantum Theory of the Electron Liquid* (Cambridge University Press, Cambridge, England, 2005).
- [25] See Supplemental Material at <http://link.aps.org/supplemental/10.1103/PhysRevLett.132.106301> for more details, which also includes Refs. [26,27].
- [26] E. Lifshitz and L. P. Pitaevskii, *Statistical Physics. Theory of the Condensed State* (Butterworth-Heinemann, Oxford, 1980).
- [27] K. Wakabayashi, K. Sasaki, T. Nakanishi, and T. Enoki, *Sci. Technol. Adv. Mater.* **11**, 054504 (2010).
- [28] T. P. Cysne, F. S. M. Guimarães, L. M. Canonico, T. G. Rappoport, and R. B. Muniz, *Phys. Rev. B* **104**, 165403 (2021).
- [29] J. Lee, K. F. Mak, and J. Shan, *Nat. Nanotechnol.* **11**, 421 (2016).